
# Resolution-Improvement of Confocal Fluorescence Microscopy via Two Different Point Spread Functions

Xuanhoi Hoang, Vannhu Le, and MinhNghia Pham(✉)

Le Quy Don Technical University, Hanoi, Vietnam
levannhuktq@gmail.com, nghiapm2018@mta.edu.vn

**Abstract.** In this paper, we propose a new method to obtain the improvement of lateral axial resolution of confocal fluorescence microscopy. In this method, we employ two different beams to illuminate the sample: (1) the Gaussian beam; (2) the donut beam. Two different images are produced from these two illumination beams. A higher resolution image is generated by a multi-relationship between these two image. A set of simulation and experimental results are employed to compare the effectiveness of proposed method with the traditional confocal fluorescence microscopy. These results demonstrated that our method can be employed to achieve the resolution-enhancement of confocal fluorescence microscopy.

**Keywords:** High-resolution · Confocal fluorescence microscopy · Image processing

## 1 Introduction

Because of the diffraction limit, the maximum spatial resolution of tradition optical microscopy in the far field is about 0.61 λ/NA, in which λ is the illumination wavelength and *NA* is the numerical aperture [1–3]. Confocal fluorescence microscopy (CFM) provides the relatively high-resolution image that has low out-of-focus background-noise. Additionally, the CFM system can be used to achieve the resolution improvement by a factor of $\sqrt{2}$ [4, 5]. Therefore, the CFM is extensively employed to analyze of three-dimensional sample and becomes a powerful tool for investigating specimen in the life science. However, the resolution of the CFM only reaches to 200 nm under the recent experimental condition [6, 7].

Note that STED nanoscopy is based on the nonlinear excitation process as for breaking Abbe's diffraction limit and yet is limited by the high intensity radiation that may cause side effects like photo-bleaching or photo-toxicity due to non-linear saturated rationale [8, 9]. In addition, another non-negligible limitation is the problem of strong background signals mostly left by secondly-excited depletion beam. Requirement for special dyes of STED is another drawback. These disadvantages give rise to the booming development of other STED-like techniques with biological compatibility, such as


N.-S. Vo and V.-P. Hoang (Eds.): INISCOM 2020, LNICST 334, pp. 77–84, 2020.
https://doi.org/10.1007/978-3-030-63083-6_6

reversible saturable optical fluorescence transitions (RESOLFT) [10], charge state depletion (CSD) [11], ground state depletion (GSD) [12], fluorescence quenching microscopy (FQM) [13], excited state saturation (ESSat) [14] and fluorescence emission difference microscopy (FED) [15] and so on. Another super-resolution strategy, applying molecular energy state difference and multiply-beam illumination, as well as thousands of times of photon acquisitions, is concerning single-molecular localization imaging (SML), like stochastic optical reconstruction microscopy (STORM) [16, 17] and photo-activated localization microscopy (PALM) [18, 19]. Tens of thousands of wide-field illumination register fluorescent dyes while each illumination only excites sparsely-distributed molecules beyond diffraction limit. Digital reconstruction of these images will result in super-resolved structures. These SML techniques are limited by the long acquisition time and the special dyes. Structured illumination microscopy (SIM) is an alternative approach to break the diffraction barrier by a factor of 2, based on multiply-beam illumination [20, 21]. By virtue of periodically patterning the illumination light with different illumination angles and light polarizations, high frequency information could be extracted through post-processing. This technique, however, is costly due to expensive architecture in order to achieve video-rate acquisition speed. In addition, the resolution improvement is also limited although saturated SIM (SSIM) could further improve the spatial resolution at the price of high risk of photo-bleaching.

In this paper, we suggest a novel approach for the improvement of resolution of confocal fluorescence microscopy. In this method, we introduce two illumination beams. The first beam is the Gaussian beam. The second beam is the donut beam which are modulated by the 0–2 vortex phase mask. For obtaining the image with the higher resolution, we introduce a multiplying relationship between the two images. The proposed method is simple and performs easily.

## 2 Methodology

By using vector diffraction theory, the intensity distribution of incident light propagating through an objective lens can be calculated. The electric field near the focus imaging plane can be acquired explicitly by the formulae derived from the Debye integral as:

$$\vec{E}(r_2, \xi_2, z_2) = iC \iint_{\Omega} \sin(\varsigma) E_0 A(\varsigma, \xi) P \times e^{i\Delta a(\varsigma,\xi)} e^{ikn(z_2 \cos\varsigma + r_2 \sin\varsigma cons(\xi - \xi_2))} d\varsigma d\xi \quad (1)$$

where $\vec{E}(r_2, \xi_2, z_2)$ represents the electric field vector at the point $(r_2, \xi_2, z_2)$ which is generated by cylindrical coordinates, $C$ shows the normalized constant, $E_0$ represents the amplitude distribution of the input light beam, $A(\zeta, \xi)$ represents a $3 \times 3$ matrix related to the structure of the imaging lens and $P$ presents Jones vector of the incident light beam. $\Delta a(\zeta, \xi)$ represents the parameter of phase delay using the phase mask.

When the sine condition is used with the object lens, $A(\zeta, \xi)$ can be represented by,

$$A(\varsigma, \xi) = \sqrt{\cos\varsigma} \begin{bmatrix} 1 + (\cos\varsigma - 1)\cos^2\xi & (\cos\varsigma - 1)\cos\xi \sin\xi & -\sin\varsigma\cos\xi \\ (\cos\varsigma - 1)\cos\xi \sin\xi & 1 + (\cos\varsigma - 1)\sin^2\xi & -\sin\varsigma\sin\xi \\ \sin\varsigma\cos\xi & \sin\varsigma\sin\xi & \cos\varsigma \end{bmatrix} \quad (2)$$

The point spread function (PSF), $h$, can be calculated through the intensity distribution as,

$$h = \left|\vec{E}\right|^2 \tag{3}$$

The image can be illuminated by the following equation

$$I = x * h \tag{4}$$

in which $x$ denotes the observation-sample.

In this paper, we introduce one method based on the use of two kinds of PSFs to achieve the improvement of the resolution of the CFM. The two images can be captured by using the two PSFs. One image is acquired by employing the dot beam which is modulated by Gaussian beam. This image is called the dot image. Other image is achieved by using the donut beam that is modulated by the 0–2 vortex phase mask as depicted in Fig. 1. This image is called the donut image. The third image is generated by using the multiplying relationship between the dot image and the donut image as shown in Fig. 2. This image is called the multi-image. The proposed image can be presented by,

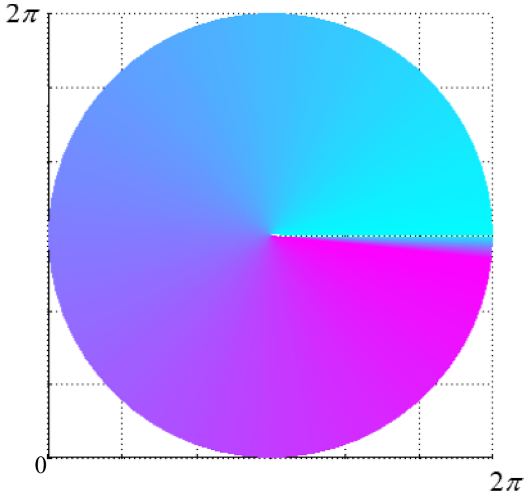


**Fig. 1.** The 0–2 vortex phase mask.

$$I = I_{Dot} \exp(\alpha./(I_{Donut} + \beta)) \tag{5}$$

We show the two feasible imaging schemes which can be used to perform the proposed method. The first model is shown in Fig. 3(a). It can be seen that two illumination paths are shown: the first path is Gaussian beam, the second path is donut one. The donut beam is modulated by 0–2π vortex phase mask that is generated by a spatial light modulator (SLM). Because two illumination paths are separated before the BS, we should

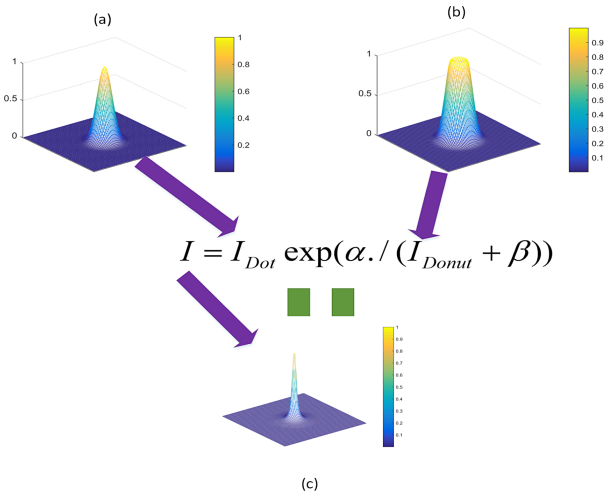


**Fig. 2.** The multi-theory. (a) the PSF is generated by the dot beam; (b) the PSF is generated by the donut beam; (c) the PSF is generated by using the multiplying relationship.

carefully adjust the two illumination beams, to protect that the two PSFs of these two beams have the same position on the sample. Other model is depicted in Fig. 3(b). In this model, a SLM is inserted to the illumination path of the optical system, which is used to switch different kinds of phase masks. When we want to use the dot beam, the SLM will generate the 0 phase mask. When we want to employ the donut beam, the SLM will produce 0–2π vortex phase mask. It can be seen that the setup of optical system in Fig. 3(b) is simpler in comparison with that in Fig. 3(a). Therefore, we use the setup of the optical system in Fig. 3(b).

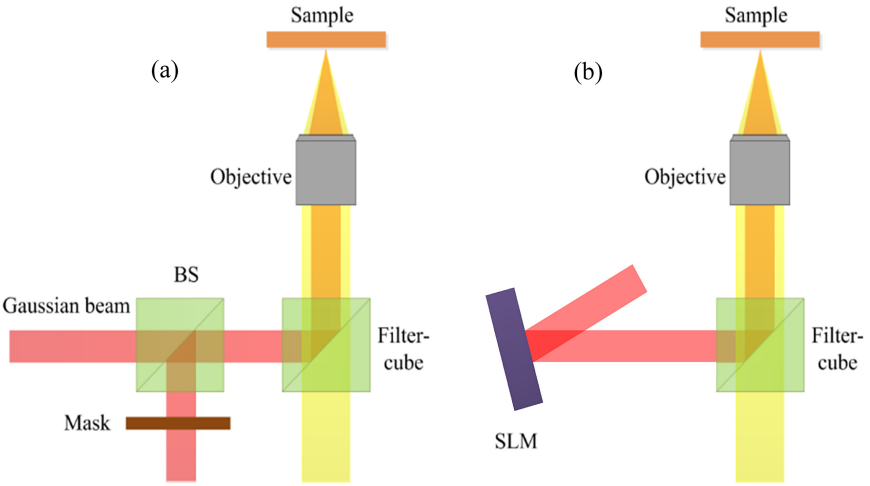


**Fig. 3.** Optical layouts via two illumination beams in CFM.

## 3 Simulation and Experimental Results

In order to highlight the proposed ability for the improvement of the resolution, we perform some simulation results. We use some initial parameters for simulation condition: $NA = 1.49$; the illumination laser, $\lambda = 640$ nm, is used to illuminate sample; the sample is placed in the medium for index refraction of 1.518. The first, we consider with the spokes image. The original image is illuminated in Fig. 4(a), its size is set to $6\lambda \times 6\lambda$. By using Eq. (4), Fig. 4(b) shows the confocal image, while the proposed image is illuminated in Fig. 4(c) with $\alpha = 5$ and $\beta = 1$. We draw additionally one blue circle one the confocal image and the proposed image. It can be seen that the outside of the blue circle, we can discern for the confocal image and the proposed image. However, the inside of the blue circle, the confocal image is not discerned, while some parts of the proposed image still discerns. This means that the effectiveness of our method for the improvement of the resolution can be achieved.

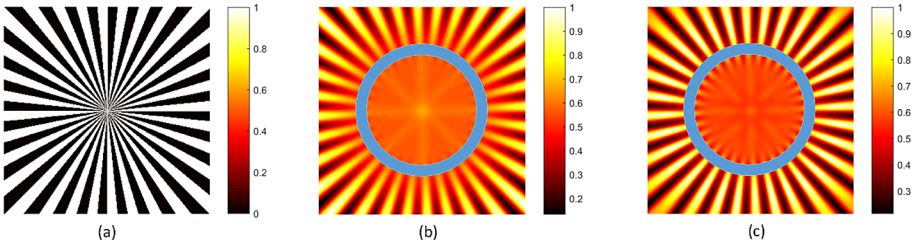


**Fig. 4.** (a) the original image; (b) the confocal image; (c) the proposed image (Color figure online)

Next, we simulate the imaging process with cell microtubules. The original image is illuminated in Fig. 5(a). The size of the original image is equal to $6\lambda \times 6\lambda$. The confocal image of the CFM is depicted in Fig. 5(b). Figure 5(c) indicates the proposed image. There are the two lines which nearly parallel at the positions (1) and (2) on the original image. It can be seen that the two lines of the confocal image which is shown at the positions (1) and (2) do not separate. While the two lines of the proposed image can be discerned.

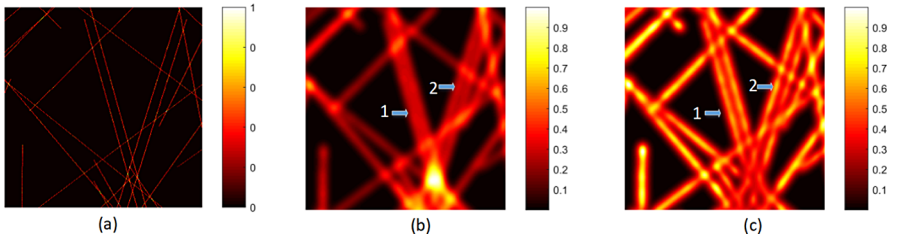


**Fig. 5.** (a) the original image; (b) the confocal image; (c) the proposed image.

The finally, in order to highlight the ability of the resolution-improvement of our method, 200 nm spherical fluorescence particles are used to perform experiment. The

experimental result of CFM is represented in Fig. 6(a). Figure 6(b) depicts the experimental result of the proposed method. It can be seen that the size of spherical fluorescence particles of two images is the near same. However, the resolution-ability of the proposed image is better than that of the confocal image. This can be clearly shown by drawing a line though the center of the particle as depicted on the Fig. 6(a) and (b). This line is illuminated in the Fig. 6(c). Form Fig. 6(c), it can be clearly seen that the resolution by using the proposed method was remarkably improved. We use full-width at half-maximum (FWHM) to measure the ability of resolution. The FWHM of the particle on the proposed image is smaller 1.43 time that that of the particle on the confocal image. This result demonstrated that our method can be used to improve the resolution of the CFM.

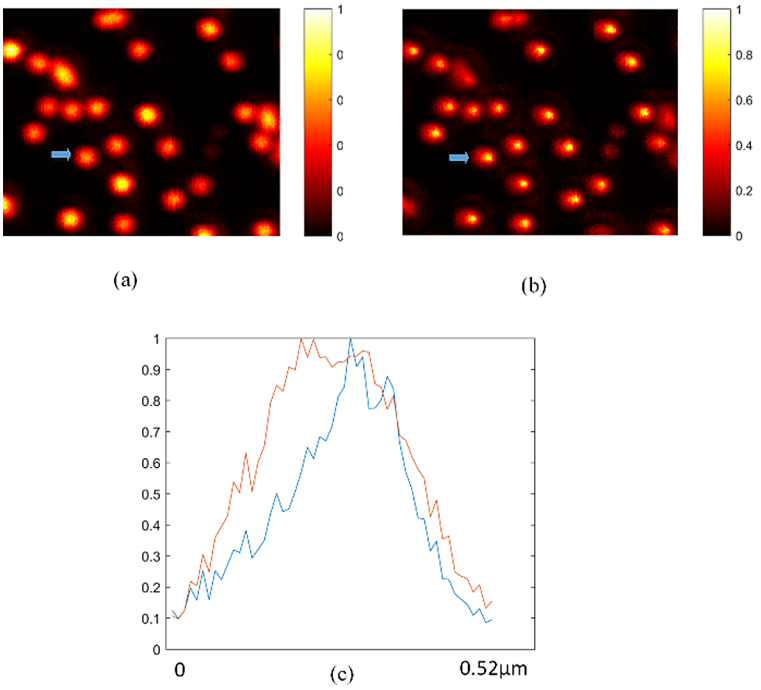


**Fig. 6.** The experimental result of (a) the confocal image; (b) the proposed image; (c) the image of one line through the center of the particle.

## 4 Conclusion

We have suggested one effective method using two PSFs to achieve the enhancement of the resolution of CFM. Two images are generated by two kinds of the PSFs. A novel relationship between these two images is built. The effectiveness of our method is demonstrated by some simulation results. The experiment with spherical fluorescence

particles was shown. The experimental result illuminated that the proposed method can be employed to acquire the improvement of the resolution about 1.43 times. The proposed method can be used in many different fluorescence microscopies such as light-sheet fluorescence microscopy, wide-field fluorescence microscopy, etc.

**Acknowledgment.** This work is supported by Vietnam National Foundation for Science and Technology Development (NAFOSTED) under Grant number (103.03-2018.08).

## References

1. Wan, C., et al.: Three-dimensional visible-light capsule enclosing perfect supersized darkness via antiresolution. Laser Photonic Rev. **5**, 743–749 (2014)
2. Pawley, J.: Handbook of Biological of Confocal Microscopy, 3rd edn. Springer, New York (2006)
3. Wilson, T.: Confocal Microscopy, vol. 426, pp. 1–64. Academic Press, London (1990)
4. Gu, M.: Principles of Three Dimensional Imaging in Confocal Microscopies. World Scientific, Singapore (1996)
5. Segawa, S., Kozawa, Y., Sato, S.: Resolution enhancement of confocal microscopy by subtraction method with vector beams. Opt. Lett. **39**(11), 3118–3121 (2014)
6. So, S., et al.: Overcoming diffraction limit: from microscopy to nanoscopy. Appl. Spectros. Rev. **53**(1) (2017)
7. Le, V., Wang, X., Kuang, C., Liu, X.: Resolution enhancement of confocal fluorescence microscopy via two illumination beams. Optics Lasers Eng. **122**, 8–13 (2019)
8. Hell, S.W., Wichmann, J.: Breaking the diffraction resolution limit by stimulated emission: stimulated-emission-depletion fluorescence microscopy. Opt. Lett. **19**, 780–782 (1994)
9. Gao, P., Prunsche, B., Zhou, L., Nienhaus, K., Nienhaus, G.U.: Background suppression in fluorescence nanoscopy with stimulated emission double depletion. Nature photonic. **11**, 163–169 (2017)
10. Wang, S., Chen, X., Chang, L., Xue, R., Duan, H., Sun, Y.: GMars-Q Enables long-term live-cell parallelized reversible saturable optical fluorescence transitions nanoscopy. ACS Nano **10**(10), 9136–9144 (2016)
11. Sharma, Reena., Singh, Manjot, Sharma, Rajesh: Recent advances in STED and RESOLFT super-resolution imaging techniques. Spectrochim. Acta Part A Mol. Biomol. Spectrosc. **231**(15), 117715 (2020)
12. Dixon, Rose E., Vivas, Oscar., Hannigan, Karen I., Dickson, Eamonn J.: Ground state depletion super-resolution imaging in mammalian cells. J. Vis. Exp. **129**, 56239 (2017)
13. Chen, X., Zou, C., Gong, Z., Dong, C., Guo, G., Sun, F.: Sub-diffraction optical manipulation of the chargestate of nitrogen vacancy center in diamond. arXiv:1410.4668
14. Trebbia, J.-B., Baby, R., Tamarat, P., Lounis, B.: 3D optical nanoscopy with excited state saturation at liquid helium temperatures. Opt. Express **27**(16), 23486–23496 (2019)
15. Li, Y., et al.: Image scanning fluorescence emission difference microscopy based on a detector array. J. Microsc. **266**, 288–297 (2017)
16. Rust, M.J., et al.: Sub-diffraction-limit imaging by stochastic optical reconstruction microscopy (STORM). Nat. Methods **3**, 793–796 (2006)
17. Huang, B., et al.: Three-dimensional super-resolution imaging by stochastic optical reconstruction microscopy. Science **319**, 810–813 (2008)
18. Betzig, E., et al.: Imaging intracellular fluorescent proteins at nanometer resolution. Science **313**, 1642–1645 (2006)

19. Hess, S.T., et al.: Ultra-high resolution imaging by fluorescence photoactivation localization microscopy. Biophys. J. **91**(11), 4258–4272 (2006)
20. Classen, A., et al.: Superresolution via structured illumination quantum correlation microscopy. Optica **4**(6), 480 (2017)
21. Gustafsson, M.G.L.: Nonlinear structured-illumination microscopy: wide-field fluorescence imaging with theorycally unlimited resolution. PNAS **102**(37), 13081–13086 (2005)